Metabolomics of colistin methanesulfonate treated *Mycobacterium tuberculosis*

Nadia Koen, S van Breda, Du Toit Loots

The first and last authors contributed equally to the writing of this manuscript

Nadia Koen
Address: North-West University (Potchefstroom Campus), Private Bag x6001, Box 269, Potchefstroom, South Africa, 2531
E-mail: nadiakoen93@gmail.com

Shane Vontelin van Breda
Address: Department of Internal Medicine, Division of Infectious Diseases, University of Pretoria, Pretoria, South Africa, 0002
E-mail: shane.vontelin.van.breda@gmail.com

Prof. Du Toit Loots
(Corresponding author)
Address: Human Metabolomics, North-West University, Private Bag x6001, Box 269, Potchefstroom, South Africa, 2531
Office: +27 (0) 18 299 1818
Fax: +27 (0) 18 299 1823

E-mail: dutoit.loots@nwu.ac.za

Abstract

Over the last 5 years, there has been a renewed interest in finding new compounds with anti-TB action. Colistin methanesulfonate or polymyxin E, is a possible anti-TB drug candidate, which may in future be used either alone or in combination to the current 6 month “directly observed treatment short-course” (DOTS) regimen. However its mechanism of action has to date not yet been fully explored, and only described from a histological and genomics perspective. Considering this, we used a GCxGC-TOFMS metabolomics approach and identified those metabolite markers characterising *Mycobacterium tuberculosis* (*Mtb*) cultured in the presence of colistin methanesulfonate, in order to better understand or confirm its mechanism of action. The metabolite markers identified indicated a flux in metabolism of the colistin methanesulfonate treated *Mtb* towards fatty acid synthesis and cell wall repair, confirming previous reports that colistin acts by disrupting the cell wall of mycobacteria. Accompanying this, is a subsequently elevated glucose uptake, since the latter now serves as the primary energy substrate for the upregulated glyoxylate cycle, and additionally as a precursor for further fatty acid synthesis via the glycerolipid metabolic pathway. Furthermore, the elevated concentrations of those metabolites associated with pentose phosphate, valine, threonine, and pentanediol metabolism, also confirms a shift towards glucose utilization for energy production, in the colistin methanesulfonate treated *Mtb*.

Keywords

Colistin methanesulfonate, *Mycobacterium tuberculosis*, Tuberculosis, Metabolomics, Treatment, Antibiotics

1. Introduction

In 2015, an approximated 10.5 million new cases of tuberculosis (TB) was reported globally, which subsequently contributed to 1.4 million deaths [1]. Tuberculosis is caused by the infectious organism *Mycobacterium tuberculosis* (*Mtb*), a mycobacteria bacillus which mainly targets the lungs [2]. Currently, the WHO approved treatment approach entails a 6 months combination treatment approach which is called the "directly observed treatment short-course" (DOTS) regimen [3]. According to the annual WHO report, a significant improvement to current treatment strategies is going to be a challenge, however the identification of new anti-TB drug candidates and or alternative treatment regimens, might be a plausible option for speeding up treatment duration and subsequently lowering the TB prevalence globally [4,5]. Although there are currently a number of new potential anti-TB drugs undergoing phase II and III preclinical trials, delamanid and bedaquiline are the only two new anti-TB drugs to have been approved over the last 50 years. These drugs, however, are currently only used for treating adults with MDR-TB, and considered as last option medications, when no other alternatives prove to be effective [6]. Considering this, there is still urgent need for new TB drugs and alternative TB treatment approaches.

Another possible anti-TB drug candidate is the antibiotic colistin methanesulfonate (CMS), an inactive prodrug of colistin sulfate (CS), also known as polymyxin E [7]. CMS has previously been shown to have high anti-bacterial activities against *P. aeruginosa*, *A. baumannii*, and *Klebsiella pneumoniae,* and additionally shown to be resistant to these organisms developing drug tolerance [8]. CMS is produced via a reaction from commercially synthesised CS with formaldehyde and sodium bisulphite, resulting in the subsequent addition of a sulfomethylated group to the primary amine groups of CS [9]. The original reason for modifying CS in this manner is that the resulting CMS is considered less toxic when administered parenterally [10]. When administered, a hydrolysis reaction occurs, where CMS in an aqueous solution forms both CS and various partially sulfomethylated derivatives of CS [11]. Apart from the varying toxicity characteristics of CS and CMS, these two forms of the drug show different pharmacokinetic characteristics [12–14]. A study conducted by Plachouras et al., 2009, indicated that colistin concentrations increase slowly after the administration of CMS in critically

ill patients, reaching a steady state after 2 days, suggesting benefits of treatment commencement with a loading dose [15]. Various colistin derivitives have also been proposed to promote first line anti-TB drug uptake, by creating pores in the outer membrane of *Mtb*, after binding electrostaticly to the outer cell membrane lipopolysaccharides and phospholipids [16]. Very little data however exists describing the antimicrobial action of CMS against *Mtb,* which has been decribed to date, was attained solely from a histologicical or genomics approach. Metabolomics, the latest addition to the "omics" family, is defined as an unbiased identification and quantification of all metabolites present in a sample, using highly specialised analytical procedures and a statistical analysis / bioinformatics, by which the most important metabolites characterising a pertubation (or drug) can be identified [17]. In this investigation, we extracted the intracellular metabolome of *Mtb* cultured in the presence and absence of 32 µg/ml CMS, and analysed these extracts using a 2 dimansional gas chromatography time of flight mass spectrometry (GCxGC-TOFMS) metabolomics approach, for the purpose of identifying those metabolite markers best characterising the changes to the *Mtb* metabolome induced by CMS.

2. Materials and methods

2.1 Cell culture

As described by van Breda et al., (2015), the cell cultures were prepared in the presence and absence of CMS, with slight modifications. Briefly, *Mtb* H37Ra ATCC 25177 (obtained from Ampath Pathology Laboratory Support Services, Centurion, Gauteng, South Africa) was swabbed onto Middlebrook 7H10 agar (Becton Dickinson, Woodmead, Gauteng, South Africa), supplemented with 0.5% v/v glycerol (Saarchem, Krugersdorp, Gauteng, South Africa), and enriched with 10% v/v oleic acid, albumin, dextrose, catalase (OADC) (Becton Dickinson). The reasons for selecting a H37Ra strain in this experiment, was due to the fact that the original description of the effects of polymyxins by Rastogi et al., (1986), used H37Ra, and a recent publication by Bax et al., (2015), described similar results using H37Rv as to what van Breda et al. (2015) described for H37Ra [16,18,19] .

The stock culture was prepared after three weeks of incubation at 37 ºC, by suspending the cells in 1 x phosphate buffered saline (PBS) (Sigma Aldrich, Kempton Park, Gauteng, South Africa) containing 0.05% v/v Tween 80 (Saarchem) to a McFarland standard of 3. Aliquots of 1 mL were stored at -80 ºC in cryovials, containing 20% v/v glycerol (Saarchem). By using the TB Ag MPT64 Device (KAT Medical, Roodepoort, Gauteng, South Africa), the presence of *Mtb* was confirmed, and the purity was determined by swabbing 100 µL of culture media onto tryptic soy agar (Merck, Darmstadt, Germany) and incubating at 37 ºC for 48 h. Before experimental investigations, a cryovial of the stored aliquots was allowed to thaw to room temperature, vortexed and swabbed onto Middlebrook 7H10 agar. Plates were sealed in Ziploc bags and incubated at 37 ºC until mid-log growth was reached (approximately 10 – 14 days).

The mid-log growth culture was suspended to a McFarland standard of 1 (using Sauton media [16]); approximately 1 x 107 colony-forming units (CFU)/mL. The cell suspension (195µL) was then added to each well in a 96 well microtiter plate (Eppendorf). The antimicrobials were added to final concentrations of 0 µg/mL and 32 µg/mL CMS respectively, and the plate was sealed using sterile ziploc bags, and incubated at 37 ºC for 24 hours. The mixture in each well was subsequently transferred to Eppendorf tubes up to a volume of 1 mL. The 10 samples containing 32 µg/mL CMS and 7 samples containing no CMS, were centrifuged at 10000 x g for 1 min and showed no difference in the amounts of viable CFU/mL. The supernatant was removed and pellet rinsed and resuspended in 1 x PBS (without Tween 80) and then stored at -80ºC.

In the current investigation it is important to note, that the reason Sauton media was used, is because other media, such as Middlebrook 7H9 for instance, contains the following components which antagonize the effects of polymyxins 1. BSA (forms complexes with polymyxins) [20], 2. Mg2+ and Ca2+ [21,22], and hence it was important to use media where physiological concentrations of these divalent cations can be controlled, i.e., cation-adjusted to 10-12.5mg Mg2+/L and 20-25mg Ca2+/L [23,24], 3. Na+ [25,26], and 4. Catalase, since the latter is an antioxidant which would inhibit polymyxin induced Fenton reaction mechanisms [27]. Furthermore, it was important to substitute glycerol with 0.2% w/v glucose, since lower than

normal MICs have been previously observed for *Mtb* when glycerol was used as the only carbon source [28], and with 0.05% v/v Tween 80, since *Mtb* requires the fatty acids present within Tween 80 for growth [29,30].

2.2 Whole metabolome extraction procedure and derivatization

Prior to GCxGC-TOFMS analysis, 0.5 mg of each of the individually cultured *Mtb* sample pellets described above were weighed into an Eppendorf tube, followed by the addition of 50 µL 3-phenylbutyric acid (0.0175µg/mL) (Sigma-Aldrich (St. Louis, MO, USA)) as internal standard. Chloroform, methanol (Burdick and Jackson brands (Honeywell International Inc., Muskegon, MI, USA)) and water were added in a ratio 1:3:1, vortexed for 1 min and then placed in a vibration mill (Retsch, Haan, Germany) with a 3 mm carbide tungsten bead (Retsch) for 5 min at 30 Hz/s. Each sample was then centrifuged for 10 min at 10 000xg and the supernatants transferred to a GC sample vial, and subsequently dried under a nitrogen stream. Each extract was derivatized using 20µL methoxyamine hydrochloride-(trimethylsilyl)-trifluoroacetamide (MSTFA) (Sigma-Aldrich (Darmstadt, Germany)) (containing 15 mg/mL pyridine) at 50 °C for 90 min, followed by silylation using 40µL MSTFA with 1 % trimethylchlorosilane (TMCS) at 50 °C for 60 min. These extracts were then transferred to a 0.1 mL insert in a clean GC sample vial and capped, prior to GCxGC-TOFMS analysis [31].

2.3 GCxGC-TOFMS analyses

The samples (1 µL) were analysed in random sequence, using a Pegasus 4D GCxGC-TOFMS (LECO Africa (Pty) Ltd, Johannesburg, South Africa), equipped with an Agilent 7890 gas chromatograph (Agilent, Atlanta, USA), TOFMS (LECO Africa) and Gerstel Multi-Purpose Sampler (Gerstel GmbH and Co. KG, Mülheim an der Ruhr, Germany), in a splitless ratio. The necessary quality control (QC) samples were also analyzed at regular intervals in order to correct for any batch effects and also monitor the performance of the analysis over time. A Rxi-5Sil MS primary capillary column (30 m, 0.25 µm film thickness and 250 µm internal diameter), and a Rxi-17 secondary capillary column (1.2 m, 0.25 µm film thickness and 250 µm internal diameter) where used for GC compound separation. Helium was used as a carrier gas at a flow of 1 mL/min with the injector temperature held constant at 270 °C for the entire run. The primary

column temperature was set at 70 °C for 2 min, and then increased at a rate of 4 °C/min to a final temperature of 300 °C, at which it was maintained for a further 2 min. The temperature of the secondary oven was programmed at 85 °C for 2 min, then increased at a rate of 4 °C/min to final temperature of 305 °C, at which it was maintained for a further 4.5 min. The acquisition voltage of the detector was 1700 V and the filament bias -70 eV. A mass range of 50–800 m/z was used for the mass spectra, at an acquisition rate of 200 spectra/s.

2.4 Data processing, clean-up and statistics

Mass spectral deconvolution (at a signal to noise ratio of 20), peak alignment and peak identification, were done on the collected mass spectra using ChromaTOF software (version 4.32). Identical mass spectra of the compounds in each of the samples were aligned, if they displayed similar retention times. Compounds were identified by comparison of their mass fragment patterns and retention times, to that of libraries compiled from previously injected standards.

Following the data processing steps described above, a standardized metabolomics data clean-up procedure was conducted [32]. Normalization of each of the detected compounds was done using the total useful MS signal (TUS) [33] and by calculating the relative concentration of each compound, using the internal standard as a reference. A 50% filter was applied in order to remove those compounds showing more than 50% zero values within both groups [34] and the QC samples used to correct for any batch effects, using quantile equating [35]. Additionally, a 50% QC coefficient of variation (CV) filter was applied [36], and all zero-values were replaced by a value determined as half of the smallest concentration (i.e. the detection limit) detected in the entire data set, as these may be due to low abundance rather than being absent [37].

The data were subsequently analysed using a variety of multi- and univariate statistical methods, using a web based software package supported by the Metabolomics Society: MetaboAnalyst (based on the statistical package “R”; version 2.10.0), and included principal components analysis (PCA) [38], partial least squares–discriminant analysis (PLS–DA) [39], a t-test and effect size calculations [40].

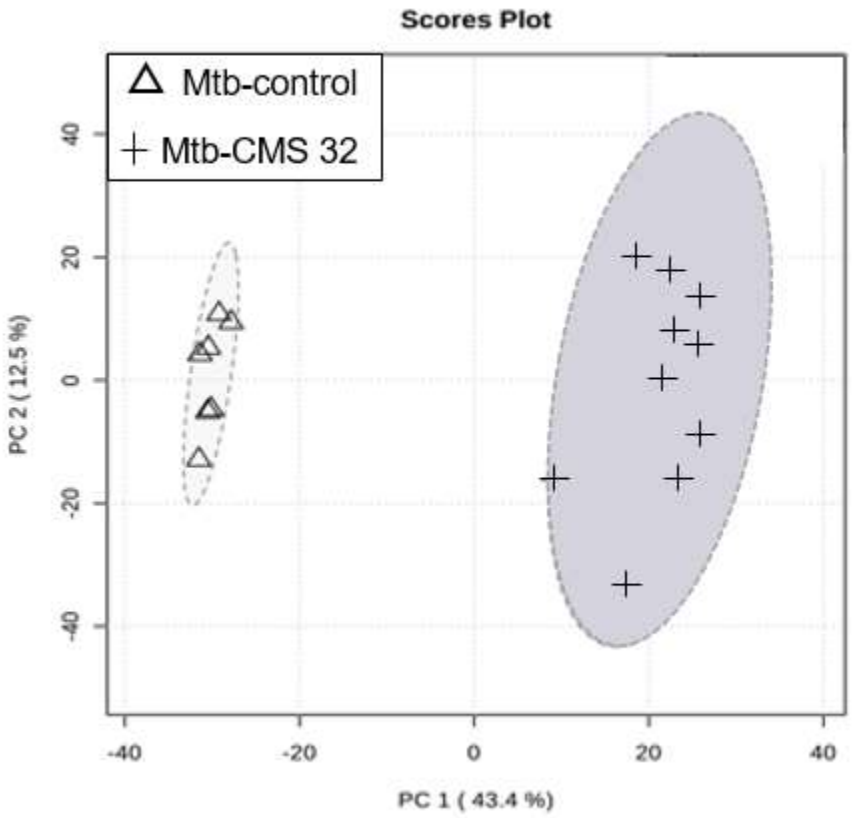

Figure 1: PCA differentiation of individually cultured *Mtb* in the absence (*Mtb*-control) and presence (*Mtb*-CMS) of colistin methanesulfonate (32 µg/mL) and analysed via GCxGC-TOFMS. The variances accounted for are indicated in parenthesis.

3. Results and Discussion

Figure 1 shows clear PCA differentiation of the individually cultured *Mtb* samples in the presence and absence of CMS, using the collected GCxGC-TOFMS metabolomics data. The total amount of variance explained by the first two principal components (PCs) (R2X cum) was 55.9%, of which PC1 accounted for 43.4%, and PC2 accounted for 12.5%. Subsequently, by compliance with all of the following criteria: a PCA modelling power > 0.5 [38], a PLS-DA VIP value > 1 [39], a t-test P-value < 0.05 and an effect size > 0.5 [40], the metabolites that contributed most to this differentiation were selected (Figure 2) and listed in Table 1. These

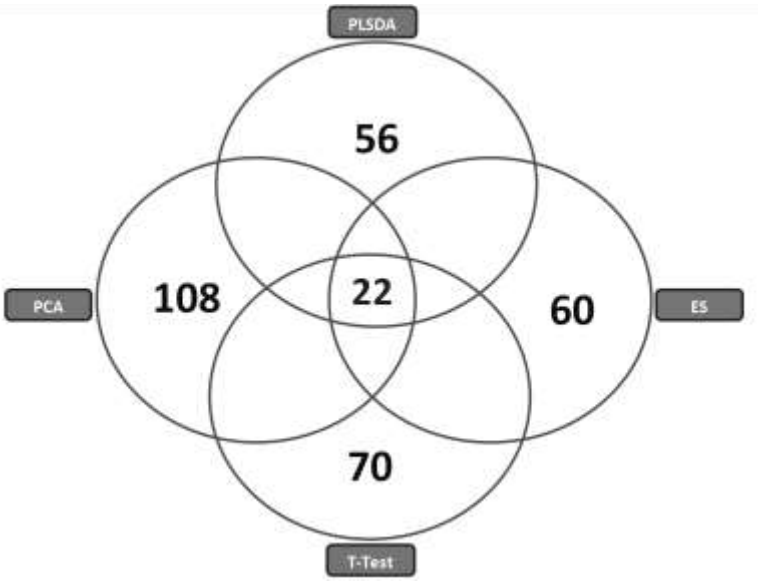

Figure 2: Venn diagram illustrating the multi-statistical selection criteria of the 22 metabolite markers best describing the variation between the individually cultured *Mtb* sample groups in the presence and absence of CMS.

Metabolite name	***Mtb* controls:**	***Mtb* controls:**	***Mtb* treated with CMS:**	***Mtb* treated with CMS:**	**PCA**	**PLS-DA**	**Effect sizes**	**t-test**	**Fold Change**
(**Chemspider ID**)	**Average concentration (mg/g cells)**	**standard error of the mean**	**Average concentration (mg/g cells)**	**standard error of the mean**	**(Power)**	**(VIP)**	**(d-value)**	**(P-value)**	**(log2)**
Tetramethylhexadecanol (92535)	0,005	0,001	0,011	0,003	0,663	1,087	2,095	0,003	1.14
Methyladipic Acid (5367266)	0,159	0,024	0,204	0,042	0,984	1,592	1,063	<0,001	0.36
Arabitol (84971)	0,554	0,133	0,328	0,062	0,989	1,603	1,703	<0,001	-0.59
Diethylene glycol (DEG) (13835180)	0,072	0,020	0,036	0,008	0,925	1,111	1,870	0,002	-1.00
Dotriacontane (10542)	0,070	0,013	0,053	0,013	0,722	1,147	1,279	0,001	-0.40
Erythrose (84990)	0,166	0,030	0,731	0,289	0,806	1,277	1,955	<0,001	2.14
Glycerol (733)	0.007	0.006	0.023	0.014	0,860	1,034	1,852	0,005	1.72
Hentriacontane (11904)	0,605	0,202	1,007	0,483	0,980	1,574	0,834	<0,001	0.74
Methyldodecanoic acid (92948)	0,045	0,011	0,097	0,010	0,987	1,582	4,830	<0,001	1.11

Methylmaleic acid (553689)	0,078	0,026	0,033	0,011	0,926	1,322	1,731	<0,001	-1.24
Methylglutaric acid (11549)	0,071	0,022	0,043	0,007	0,844	1,184	1,287	0,001	-0.72
Methyltetradecanoic acid (90098)	0,317	0,021	0,840	0,302	0,799	1,010	1,731	0,007	1.41
Monopalmitin (110006)	0,165	0,058	0,220	0,063	0,935	1,472	0,873	<0,001	0.42
Octacosane (11902)	0,046	0,017	0,087	0,035	0,921	1,318	1,201	<0,001	0.92
Octadecane (11145)	0,020	0,011	0,077	0,024	0,982	1,571	2,364	0,000	1.95
Octadecenoic acid (393217)	<0,001	<0,001	0,010	0,009	0,925	1,467	1,125	<0,001	3.32
Octanoic acid (370)	0,204	0,192	0,019	0,013	0,903	1,273	0,969	<0,001	-3.43
Oxalate (946)	0,027	0,008	0,113	0,020	0,986	1,572	4,247	<0,001	2.07
Pentanediol (133167)	0,014	0,013	0,028	0,008	0,965	1,580	1,033	<0,001	1.00
Tetradecanol (10714572)	0,016	0,003	0,047	0,013	0,991	1,482	2,380	<0,001	1.56
Threonine (6051)	<0,001	<0,001	0,007	0,008	0,859	1,229	0,891	<0,001	2.81
Valine (6050)	<0,001	<0,001	0,033	0,041	0,872	1,272	0,822	<0,001	5.04

Table 1: The 22 metabolite markers best explaining the variance between the individually cultured *Mtb* samples in the absence (*Mtb*-Controls) and presence (*Mtb*-CMS) of colistin methanesulfonate.

metabolite markers were mapped on a metabolic chart as indicated in Figure 3 and discussed below. As indicated, the metabolomics investigation of the cultured *Mtb* in the presence and absence of CMS, led to the identification of various significantly altered metabolite markers. Glucose uptake was increased in the CMS treated *Mtb*, as the preferential energy source (as opposed to fatty acids which are now preferentially being used for cell wall repair) to fuel an upregulated glyoxylate cycle, and substrate further cell wall fatty acid synthesis via the glycerolipid metabolic pathway. However, the CMS treated *Mtb*, also showed comparatively elevated metabolites associated with pentose phosphate, valine, threonine, and pentanediol metabolism. These results confirm that CMS disrupts the *Mtb* cell membrane, and that these bacteria attempt to compensate for this via upregulation of various metabolic pathways related to cell wall repair.

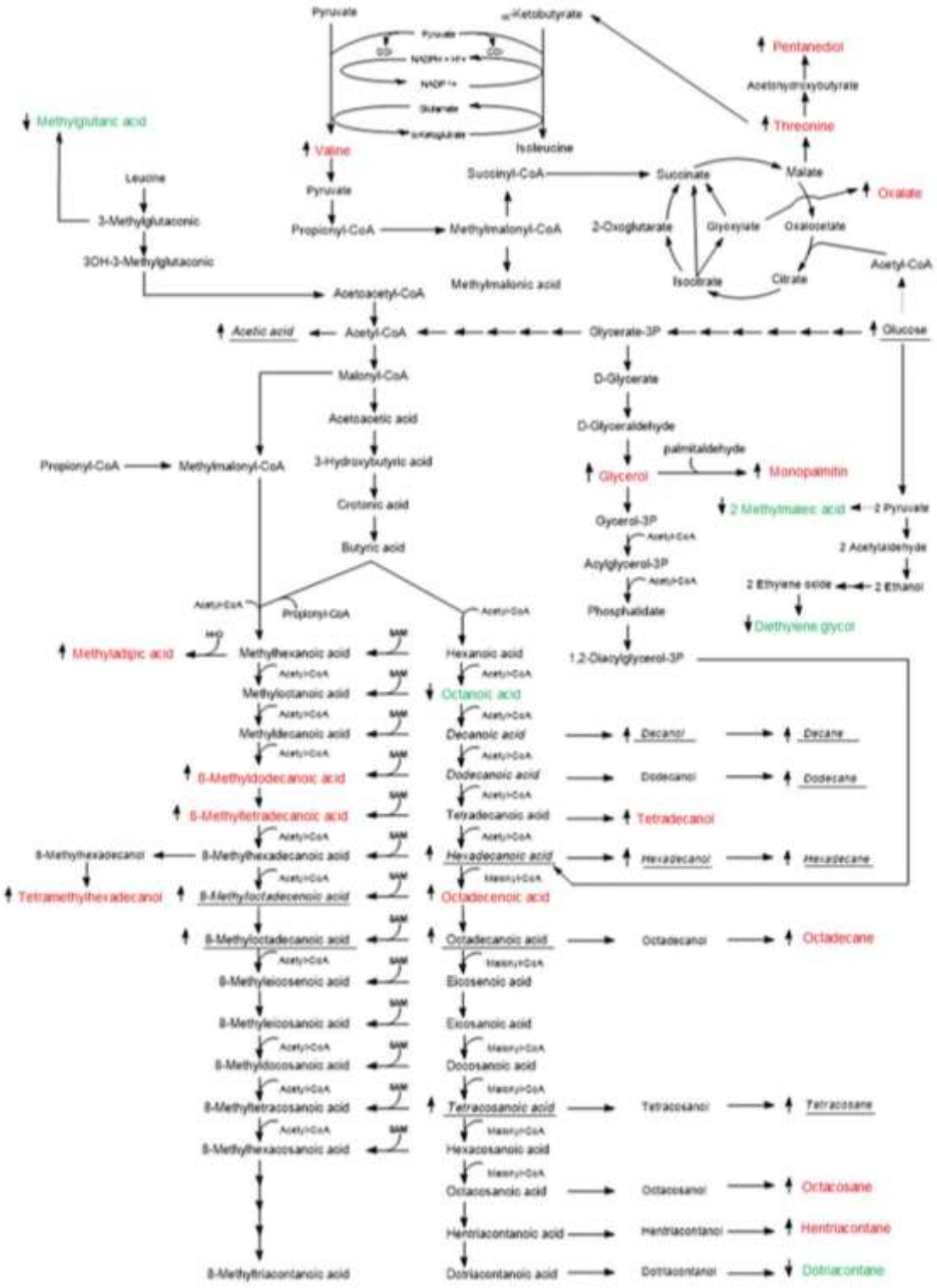
Pyruvate
α-Ketobutyrate
Pentanediol
Acetohydroxybutyrate
Threonine
Methylglutaric acid
Valine
Isoleucine
Succinyl-CoA
Succinate
Malate
Oxalate
Leucine
Pyruvate
3-Methylglutaconic
Propionyl-CoA
Methylmalonyl-CoA
2-Oxoglutarate
Glyoxylate
Oxaloacetate
3OH-3-Methylglutaconic
Methylmalonic acid
Isocitrate
Citrate
Acetyl-CoA
Acetoacetyl-CoA
Acetic acid
Acetyl-CoA
Glycerate-3P
Glucose
Malonyl-CoA
D-Glycerate
Acetoacetic acid
D-Glyceraldehyde
palmitaldehyde
Propionyl-CoA
Methylmalonyl-CoA
3-Hydroxybutyric acid
Glycerol
Monopalmitin
2 Methylmaleic acid
2 Pyruvate
Crotonic acid
Glycerol-3P
2 Acetylaldehyde
Butyric acid
Acyglycerol-3P
2 Ethylene oxide
2 Ethanol
Phosphatidate
Diethylene glycol
Methyladipic acid
Methylhexanoic acid
Hexanoic acid
1,2-Diacylglycerol-3P
Methyloctanoic acid
Octanoic acid
Methyldecanoic acid
Decanoic acid
Decanol
Decane
8-Methyldodecanoic acid
Dodecanoic acid
Dodecanol
Dodecane
8-Methyltetradecanoic acid
Tetradecanoic acid
Tetradecanol
8-Methylhexadecanoic acid
Hexadecanoic acid
Hexadecanol
Hexadecane
8-Methylhexadecanol
Tetramethylhexadecanol
8-Methyloctadecenoic acid
Octadecenoic acid
8-Methyloctadecanoic acid
Octadecanoic acid
Octadecanol
Octadecane
8-Methyleicosenoic acid
Eicosenoic acid
8-Methyleicosanoic acid
Eicosanoic acid
8-Methyldocosanoic acid
Docosanoic acid
8-Methyltetracosanoic acid
Tetracosanoic acid
Tetracosanol
Tetracosane
8-Methylhexacosanoic acid
Hexacosanoic acid
Octacosanoic acid
Octacosanol
Octacosane
Hentriacontanoic acid
Hentriacontanol
Hentriacontane
8-Methyltriacontanoic acid
Dotriacontanoic acid
Dotriacontanol
Dotriacontane

Figure 3: Metabolite markers best describing the variation in the metabolome of the CMS treated *Mtb* compared to that of *Mtb* cultured without CMS, are schematically represented in bold and those metabolites which were not necessarily significantly elevated using the statistical procedure selected, but still showed significance via considering their P-values, indicated in italics and underlined. Elevated and reduced concentrations of each metabolite marker indicated by either ↑ or ↓ and red and green respectively.

Colistin has been previously reported to have a antimicrobial activity, which function by binding electrostatically to the lipopolysaccharides and phospholipids on the outer cell membrane of these gram negative bacteria, subsequently displacing the membrane cations (magnesium and calcium) from the phosphate groups of their membrane lipids, subsequently creating pores, which results in cell death [41]. This was supported by our previous metabolomics work on the topic, which showed that elevated fatty acid synthesis and cell wall repair mechanisms are activated in the CS treated *Mtb* [42]. As previously described by Bax, et al. (2015) and van Breda, et al. (2015), the CMS used in the current investigation, also forms colistin once administered, and hence, would also be expected to result in a structural disruption of the *Mtb* cell wall via the same mechanism as to when CS is administered. This is supported by the elevated levels of the cell wall associated with methylated and unmethylated fatty acids (methyladipic acid, methyldodecanoic acid, methyltridecanoic, octadecenoic acid) and their fatty acid associated alcohols and alkanes [43] (tetramethylhexanedecanol, octacosane, octadecane, tetradecanol, and hentriacontane (Table 1). Additionally, although not selected using the markers selection statistics approach defined in the methods section, methyloctadecenoic acid (0.49 vs. 0.42 µg/ml; $P > 0.05$), hexadecanoic acid (0.859 vs. 0.857 µg/ml; $P > 0.05$), octadecanoic acid (22.45 vs. 8.07 µg/ml; $P > 0.05$), tetracosanoic acid (24.54 vs. 14.15 µg/ml; $P > 0.05$), decanol (0.02 vs. 0.00 µg/ml; $P > 0.05$), hexadecanol (0.001 vs. 0.000 µg/ml; $P > 0.05$), decane (0.009 vs. 0.006 µg/ml; $P > 0.05$), dodecane (0.006 vs. 0.00 µg/ml; $P > 0.05$), hexadecane (0.011 vs. 0.002 µg/ml; $P > 0.05$) and tetracosane (0.018 vs. 0.00 µg/ml; $P > 0.05$), were also significantly elevated in the CMS treated *Mtb* comparatively, when considering their P-values, further supporting this mechanism (Figure 3). Octanoic acid and octadecenoic acid, are the well-known substrates for the synthesis of methylated-branched chain fatty acids and mycolic acids, both important components of arabinogalactan (AG) in the cell wall of *Mtb* [44,45]. These methylated branched fatty acids additionally serve as

hydrophobic modulators for the host's cellular immune system, and are also considered virulence factors in the microbe [46]. As indicated in Figure 3, these methylated cell wall intermediates are synthesised via 3 possible routes: 1. fatty acid methylation via S-adenosylmethionine (SAM) functioning as the methyl donor [45], 2. methylmalonyl-CoA derived polyketide synthase complexes, originating from propionyl-CoA and malonyl-CoA [47] and 3. acetyl-CoA metabolism to butyric acid, which in turn reacts with propionyl-CoA [48]. Additionally, methyladipic acid was found elevated, which is formed from methylhexanoic acid, one of the metabolites in the branched fatty acid synthesis pathways of *Mtb* [49].

Similarly as to what we previously saw for the CS treated *Mtb* [42], glycolysis and its associated pathways are also upregulated in the CMS treated *Mtb*. In our previous metabolomics investigation using CS treated *Mtb*, elevated levels of glucose, acetic acid and oxalic acid where detected [50]. This suggests that the CS treated *Mtb* needed to preferably utilize fatty acids towards cell wall repair, and subsequently these organisms need to resort to glucose (which was freely available in the growth media) as the primary energy substrate [51]. Similarly, in the CMS treated *Mtb* in the current investigation, elevated levels of oxalate were also detected (Table 1) in addition to elevated glucose (1.21 vs. 0.88 µg/ml; $P > 0.05$) and acetic acid (0.218 vs. 0.102 µg/ml; $P > 0.05$) when considering significance using the latter two compounds P-values. Additional evidence supporting this and indicated in Table 1 and Figure 3, where elevated levels of valine, threonine, and pentanediol, which also suggests a shift towards glucose utilization for energy and fatty acid synthesis in the CMS treated *Mtb*. Furthermore, the elevated levels of acetic acid (or acetyl-CoA) can subsequently result in the elevated synthesis of threonine and pentanediol, detected in the CMS treated *Mtb* [52]. Also associated directly with this pathway, is elevated valine synthesis from pyruvate [53], which feeds into the tricarboxylic acid (TCA) cycle via succinate [54]. Another branch chain amino acid metabolic pathway affected by CMS in *Mtb* is that of leucine's catabolism to acetyl-CoA, and the reduced amounts of 3-methylgluturic acid attests to an increased flux in this direction [55] and the subsequent synthesis of cell wall fatty acids or energy [56]. The reduced concentrations of methylmaleic acid [57] and diethylene glycol in the CMS treated *Mtb*, serve as further confirmation for the flux of glucose utilisation for growth and fatty acid synthesis via glycerol

and monopalmitin, both of which were elevated in the CMS treated *Mtb* comparatively (Table 1 and Figure 3).

An interesting observation in the CMS treated *Mtb*, where two metabolite markers associated with the pentose phosphate pathway namely, a reduced arabinose and an elevated erythrose (Table 1). As indicated in the supplementary figures, due to the high demand in fatty acid synthesis for cell repair, and an increased demand for this and energy production via glycolysis, the pentose phosphate pathways is most likely additionally utilised during such conditions for generating more intermediates for glycolysis [58], with the reduction in arabitol and elevated levels of erythrose, indicating a metabolic flux towards glyceraldehyde-3-phosphate and fructose-6-phosphate synthesis, something which wasn't previously seen in the CS treated *Mtb* [59]. A study conducted by Henry et al. (2015), indicated differentiation of gene expression following colistin treatment. These results are consistent with that found in the current study, which also suggests that colistin treatment alters the outer membrane composition and results in subsequent damage to the outer membrane of *Mtb*, as previously described [60].

Additionally, the alterations made by CMS to the *Mtb* cell membrane, results in it becoming less hydrophobic, hence it could be suggested that CMS be used in synergy with other hydrophilic drugs, which previously struggle to cross these bacterial membranes. This has been previously observed by Bax et al. (2015) and van Breda et al (2015). It is possible that disruption of the hydrophobic barrier of *Mtb* by INH (inhibiting mycolic acid synthesis) or CS from CMS could lead to a greater uptake via the self-promoted uptake for CS causing a synergistic effect. In the case of INH, disruption of the hydrophobic barrier can lead to an uptake of hydrophilic INH. According to Nasiruddin, Neyaz, & Das (2017), a promising drug delivery model could be to encapsulate the hydrophilic drugs to be carried over the membrane, however in synergy with CMS, this may no longer be required [61]. Proof for this hypothesis, are the results by Al-Shaer, Nazer, & Kherallah (2014), where a combination therapy approach of rifampicin and CMS was used against MDR *A. baumannii*, which resulted in the successful treatment of 64% of the patients, with very little side effects reported [62]. Unfortunately, the results of these

investigations are limited and no effect is given on the clinical outcomes of rifampicin induced - hepatotoxicity.

4. Concluding remarks

The most significant metabolite markers identified in this investigation, were the elevated fatty acids indicating a shift towards fatty acid synthesis and cell wall repair in the CMS treated *Mtb*. This is accompanied by an increase in glucose utilisation for energy and an additional flux towards the upregulation of the glyoxylate cycle (a precursor for cell wall fatty acids via the glycerolipid metabolic pathway), similarly to what was previously seen when treating *Mtb* with CS. Further confirmation of this shift of glucose as an energy source, and unique to this investigation is the utilization of the pentose phosphate, valine, threonine, and pentanediol pathways for this purpose. Considering this, it might be possible to use CMS with other first or second line anti-TB drugs (likely only hydrophilic ones). The feasibility, however, to treat both drug sensitive and MDR-TB using lower drug concentrations is subject to clinical trials as it is not known if CMS would be able to successfully target intracellular *Mtb*.

Funding

This research did not receive any specific grant from funding agencies in the public, commercial, or not-for-profit sectors. Prof. Anton Stoltz and Prof. Ed Nardell are specifically thanked for their funding towards the cell cultures. The North West University is thanked for financial assistance of the research which forms part of a master's study.

Transparency declarations

None to declare.

References

[1] World Health Organization, Global Tuberculosis Report 2015, 2015. http://apps.who.int/iris/bitstream/10665/191102/1/9789241565059%7B_%7Deng.pdf?ua=1.

[2] WHO, Global Tuberculosis Report 2014, WHO Rep. 2014 (2014) 171. doi:10.1155/2014/187842.

[3] M. Palmer, A. Chan, T. Dieckmann, J. Honek, Notes to biochemical pharmacology, John Wiley & Sons, 2013.

[4] R.S. Wallis, M. Maeurer, P. Mwaba, J. Chakaya, R. Rustomjee, G.B. Migliori, B. Marais, M. Schito, G. Churchyard, S. Swaminathan, Tuberculosis—advances in development of new drugs, treatment regimens, host-directed therapies, and biomarkers, Lancet Infect. Dis. 16 (2016) e34–e46.

[5] J.M. Clain, P. Escalante, Novel Treatments for Drug-Resistant Tuberculosis, Clin. Med. Insights Ther. 8 (2016) CMT-S18560.

[6] A. Zumla, P. Nahid, S.T. Cole, Advances in the development of new tuberculosis drugs and treatment regimens, Nat. Rev. Drug Discov. 12 (2013) 388–404. doi:10.1038/nrd4001.

[7] J.K. Ortwine, K.S. Kaye, J. Li, J.M. Pogue, Colistin: understanding and applying recent pharmacokinetic advances, Pharmacother. J. Hum. Pharmacol. Drug Ther. 35 (2015) 11–16.

[8] C.R. Catchpole, J.M. Andrews, N. Brenwald, R. Wise, A reassessment of the in-vitro activity of colistin sulphomethate sodium, J. Antimicrob. Chemother. 39 (1997) 255–260. doi:10.1093/jac/39.2.255.

[9] M. Barnett, S.R.M. Bushby, S. Wilkinson, Sodium sulphomethyl derivatives of polymyxins, Br. J. Pharmacol. Chemother. 23 (1964) 552–574. http://www.ncbi.nlm.nih.gov/pmc/articles/PMC1704012/.

[10] E.G. Beveridge, A.J. Martin, Sodium sulphomethyl derivatives of polymyxins., Br. J. Pharmacol. Chemother. 29 (1967) 125–135. http://www.ncbi.nlm.nih.gov/pmc/articles/PMC1557203/.

[11] J. Li, R.W. Milne, R.L. Nation, J.D. Turnidge, K. Coulthard, Stability of colistin and colistin methanesulfonate in aqueous media and plasma as determined by high-performance liquid chromatography, Antimicrob. Agents Chemother. 47 (2003) 1364–1370.

[12] J. Li, K. Coulthard, R. Milne, R.L. Nation, S. Conway, D. Peckham, C. Etherington, J. Turnidge, Steady-state pharmacokinetics of intravenous colistin methanesulphonate in patients with cystic fibrosis, J. Antimicrob. Chemother. 52 (2003) 987–992.

[13] J. Li, R.W. Milne, R.L. Nation, J.D. Turnidge, T.C. Smeaton, K. Coulthard, Pharmacokinetics of colistin methanesulphonate and colistin in rats following an intravenous dose of colistin methanesulphonate, J. Antimicrob. Chemother. 53 (2004) 837–840.

[14] J. Li, C.R. Rayner, R.L. Nation, R. Deans, R. Boots, N. Widdecombe, A. Douglas, J. Lipman, Pharmacokinetics of colistin methanesulfonate and colistin in a critically ill patient receiving continuous venovenous hemodiafiltration, Antimicrob. Agents Chemother. 49 (2005) 4814–4815.

[15] D. Plachouras, M. Karvanen, L.E. Friberg, E. Papadomichelakis, A. Antoniadou, I. Tsangaris, I. Karaiskos, G. Poulakou, F. Kontopidou, A. Armaganidis, Population pharmacokinetic analysis of colistin methanesulfonate and colistin after intravenous administration in critically ill patients with infections caused by gram-negative bacteria, Antimicrob. Agents Chemother. 53 (2009) 3430–3436.

[16] S.V. Van Breda, A. Buys, Z. Apostolides, E.A. Nardell, A.C. Stoltz, The antimicrobial effect of colistin methanesulfonate on Mycobacterium tuberculosis in vitro, Tuberculosis. 95 (2015) 440–446.

[17] J.M. Berg, J.L. Tymoczko, L. Stryer, Metabolism: basic concepts and design, Biochem. (6th Ed.), New York Free. WH Co. (2007) 428–429.

[18] N. Rastogi, M.-C. Potar, H.L. David, Antimycobacterial spectrum of colistin (polymixin E), in: Ann. l'Institut Pasteur/Microbiologie, Elsevier, 1986: pp. 45–53.

[19] H.I. Bax, J.E.M. de Steenwinkel, M.T. Ten Kate, A. van der Meijden, A. Verbon, I.A.J.M. Bakker-Woudenberg, Colistin as a potentiator of anti-TB drug activity against Mycobacterium tuberculosis, J. Antimicrob. Chemother. 70 (2015) 2828—2837. doi:10.1093/jac/dkv194.

[20] Z. Liu, K.E.J. Tyo, J.L. Martínez, D. Petranovic, J. Nielsen, Different expression systems for production of recombinant proteins in Saccharomyces cerevisiae, Biotechnol. Bioeng. 109 (2012) 1259–1268.

[21] C.-C.H. Chen, D.S. Feingold, Locus of divalent cation inhibition of the bactericidal action of polymyxin B, Antimicrob. Agents Chemother. 2 (1972) 331–335.

[22] G.F. D'amato, R. Capineri, P. Marchi, Analisi della fluorescenza da quinacrina nel complemento cromosomico di Tragopogon porrifolius L., T. eriospermus Ten., T. crocifolius L. e di Geropogon glaber L.(Compositae), Ann Bot Rome. (1977).

[23] M.E. Falagas, S.K. Kasiakou, L.D. Saravolatz, Colistin: the revival of polymyxins for the management of multidrug-resistant gram-negative bacterial infections, Clin. Infect. Dis. 40 (2005) 1333–1341.

[24] D. Landman, C. Georgescu, D.A. Martin, J. Quale, Polymyxins revisited, Clin. Microbiol. Rev. 21 (2008) 449–465.

[25] R.E.W. Hancock, H.-G. Sahl, Antimicrobial and host-defense peptides as new anti-infective

therapeutic strategies, Nat. Biotechnol. 24 (2006) 1551.

[26] S. Ramón-García, R. Mikut, C. Ng, S. Ruden, R. Volkmer, M. Reischl, K. Hilpert, C.J. Thompson, Targeting Mycobacterium tuberculosis and other microbial pathogens using improved synthetic antibacterial peptides, Antimicrob. Agents Chemother. (2013) AAC-00175.

[27] T.R. Sampson, X. Liu, M.R. Schroeder, C.S. Kraft, E.M. Burd, D.S. Weiss, Rapid killing of Acinetobacter baumannii by polymyxins is mediated by a hydroxyl radical death pathway, Antimicrob. Agents Chemother. 56 (2012) 5642–5649.

[28] K. Pethe, P.C. Sequeira, S. Agarwalla, K. Rhee, K. Kuhen, W.Y. Phong, V. Patel, D. Beer, J.R. Walker, J. Duraiswamy, J. Jiricek, T.H. Keller, A. Chatterjee, M.P. Tan, M. Ujjini, S.P.S. Rao, L. Camacho, P. Bifani, P.A. Mak, I. Ma, S.W. Barnes, Z. Chen, D. Plouffe, P. Thayalan, S.H. Ng, M. Au, B.H. Lee, B.H. Tan, S. Ravindran, M. Nanjundappa, X. Lin, A. Goh, S.B. Lakshminarayana, C. Shoen, M. Cynamon, B. Kreiswirth, V. Dartois, E.C. Peters, R. Glynne, S. Brenner, T. Dick, A chemical genetic screen in Mycobacterium tuberculosis identifies carbon-source-dependent growth inhibitors devoid of in vivo efficacy, Nat. Commun. 1 (2010) 1–8. doi:10.1038/ncomms1060.

[29] W.B. Schaefer, C.W. Lewis, Effect of oleic acid on growth and cell structure of mycobacteria, J. Bacteriol. 90 (1965) 1438–1447.

[30] M. Smith, J. Zahnley, D. Pfeifer, D. Goff, Growth and cholesterol oxidation by Mycobacterium species in Tween 80 medium., Appl. Environ. Microbiol. 59 (1993) 1425–1429.

[31] R.J. Meissner-Roloff, G. Koekemoer, R.M. Warren, D.T. Loots, A metabolomics investigation of a hyper- and hypo-virulent phenotype of Beijing lineage M. tuberculosis, Metabolomics. 8 (2012) 1194–1203. doi:10.1007/s11306-012-0424-6.

[32] I. Smuts, F.H. Van der Westhuizen, R. Louw, L.J. Mienie, U.F.H. Engelke, R.A. Wevers, S. Mason, G. Koekemoer, C.J. Reinecke, Disclosure of a putative biosignature for respiratory chain disorders through a metabolomics approach, Metabolomics. 9 (2013) 379–391.

[33] Y. Chen, G. Shen, R. Zhang, J. He, Y. Zhang, J. Xu, W. Yang, X. Chen, Y. Song, Z. Abliz, Combination of injection volume calibration by creatinine and MS signals' normalization to overcome urine variability in LC-MS-based metabolomics studies, Anal. Chem. 85 (2013) 7659–7665.

[34] N.W. Lutz, J. V Sweedler, R.A. Wevers, Methodologies for metabolomics: experimental strategies and techniques, Cambridge University Press, 2013.

[35] S.-Y. Wang, C.-H. Kuo, Y.J. Tseng, Batch Normalizer: a fast total abundance regression calibration method to simultaneously adjust batch and injection order effects in liquid chromatography/time-of-flight mass spectrometry-based metabolomics data and comparison with current calibration met, Anal. Chem. 85 (2012) 1037–1046.

[36] J. Godzien, V. Alonso-Herranz, C. Barbas, E.G. Armitage, Controlling the quality of metabolomics data: new strategies to get the best out of the QC sample, Metabolomics. 11 (2015) 518–528.

[37] P.S. Gromski, Y. Xu, H.L. Kotze, E. Correa, D.I. Ellis, E.G. Armitage, M.L. Turner, R. Goodacre, Influence of missing values substitutes on multivariate analysis of metabolomics data, Metabolites. 4 (2014) 433–452.

[38] R. Tauler, B. Walczak, S.D. Brown, Comprehensive chemometrics: chemical and biochemical data analysis, Elsevier, 2009.

[39] H.-W. Cho, S.B. Kim, M.K. Jeong, Y. Park, N. Miller, T. Ziegler, D. Jones, Discovery of metabolite features for the modelling and analysis of high-resolution NMR spectra, Int. J. Data Min.

Bioinform. 2 (2008) 176–192.

[40] M.H. Smith, A Sample/Population Size Activity: Is it the sample size of the sample as a fraction of the population that matters?, J. Stat. Educ. 12 (2004).

[41] M.E. Falagas, K.Z. Vardakas, ANTIMICROBIAL ACTIVITY, (n.d.).

[42] N. Koen, S. van Breda, Elucidating the antimicrobial mechanisms of colistin sulfate on Mycobacterium tuberculosis using metabolomics, Tuberculosis. (2018).

[43] M.-O. Park, New pathway for long-chain n-alkane synthesis via 1-alcohol in Vibrio furnissii M1, J. Bacteriol. 187 (2005) 1426–1429.

[44] D. Kaur, M.E. Guerin, H. Škovierová, P.J. Brennan, M. Jackson, Biogenesis of the cell wall and other glycoconjugates of Mycobacterium tuberculosis, Adv. Appl. Microbiol. 69 (2009) 23–78.

[45] I. du Preez, D.T. Loots, Altered fatty acid metabolism due to rifampicin-resistance conferring mutations in the rpoB Gene of Mycobacterium tuberculosis: mapping the potential of pharmaco-metabolomics for global health and personalized medicine., OMICS. 16 (2012) 596–603. doi:10.1089/omi.2012.0028.

[46] W. Lee, B.C. VanderVen, R.J. Fahey, D.G. Russell, Intracellular Mycobacterium tuberculosis exploits host-derived fatty acids to limit metabolic stress, J. Biol. Chem. 288 (2013) 6788–6800.

[47] W.R.H. Duncan, G.A. Garton, Differences in the proportions of branched-chain fatty acids in subcutaneous triacylglycerols of barley-fed ruminants, Br. J. Nutr. 40 (1978) 29–33.

[48] L.K. Massey, J.R. Sokatch, R.S. Conrad, Branched-chain amino acid catabolism in bacteria., Bacteriol. Rev. 40 (1976) 42–54. http://www.ncbi.nlm.nih.gov/pmc/articles/PMC413937/.

[49] M. Labet, W. Thielemans, Synthesis of polycaprolactone: a review, Chem. Soc. Rev. 38 (2009)

3484–3504.

[50] S. Coad, B. Friedman, R. Geoffrion, Understanding urinalysis: clues for the obstetrician–gynecologist, Expert Rev. Obstet. Gynecol. 7 (2012) 269–279.

[51] A.C. Badejo, C.W. Choi, A.O. Badejo, K.H. Shin, J.H. Hyun, Y.G. Lee, S. il Kim, K.S. Park, S.H. Kim, K.H. Jung, Y.H. Chung, Y.G. Chai, A global proteome study of Mycobacterium gilvum PYR-GCK grown on pyrene and glucose reveals the activation of glyoxylate, shikimate and gluconeogenetic pathways through the central carbon metabolism highway, Biodegradation. 24 (2013) 741–752. doi:10.1007/s10532-013-9622-9.

[52] R. Badr, C. CHASSAGNOLE, T. LETELLIER, J.-P. MAZAT, Threonine synthesis from aspartate in Escherichia coli cell-free extracts: pathway dynamics, Biochem. J. 356 (2001) 425–432.

[53] A. Kochevenko, A.R. Fernie, The genetic architecture of branched-chain amino acid accumulation in tomato fruits, J. Exp. Bot. 62 (2011) 3895–3906.

[54] A. Guleria, A. Pratap, D. Dubey, A. Rawat, S. Chaurasia, E. Sukesh, S. Phatak, S. Ajmani, U. Kumar, C.L. Khetrapal, NMR based serum metabolomics reveals a distinctive signature in patients with Lupus Nephritis, Sci. Rep. 6 (2016) 35309.

[55] G. Leipnitz, B. Seminotti, J. Haubrich, M.B. Dalcin, K.B. Dalcin, A. Solano, G. de Bortoli, R.B. Rosa, A.U. Amaral, C.S. Dutra-Filho, Evidence that 3-hydroxy-3-methylglutaric acid promotes lipid and protein oxidative damage and reduces the nonenzymatic antioxidant defenses in rat cerebral cortex, J. Neurosci. Res. 86 (2008) 683–693.

[56] S.B. Wortmann, L.A. Kluijtmans, U.F.H. Engelke, R.A. Wevers, E. Morava, The 3-methylglutaconic acidurias: what's new?, J. Inherit. Metab. Dis. 35 (2012) 13–22.

[57] R.M. Drevland, A. Waheed, D.E. Graham, Enzymology and evolution of the pyruvate pathway to 2-oxobutyrate in Methanocaldococcus jannaschii, J. Bacteriol. 189 (2007) 4391–4400.

[58] K.Y. Mi, C. Han-Saem, J.G. Yeol, P.J. Moon, Engineering the pentose phosphate pathway to improve hydrogen yield in recombinant Escherichia coli, Biotechnol. Bioeng. 108 (2011) 2941–2946. doi:10.1002/bit.23259.

[59] M.M.C. Wamelink, E.A. Struys, C. Jakobs, The biochemistry, metabolism and inherited defects of the pentose phosphate pathway: a review, J. Inherit. Metab. Dis. 31 (2008) 703–717.

[60] R. Henry, B. Crane, D. Powell, D. Deveson Lucas, Z. Li, J. Aranda, P. Harrison, R.L. Nation, B. Adler, M. Harper, The transcriptomic response of Acinetobacter baumannii to colistin and doripenem alone and in combination in an in vitro pharmacokinetics/pharmacodynamics model, J. Antimicrob. Chemother. 70 (2015) 1303–1313.

[61] M. Nasiruddin, M. Neyaz, S. Das, Nanotechnology-Based Approach in Tuberculosis Treatment, Tuberc. Res. Treat. 2017 (2017).

[62] M. Al-Shaer, L.H. Nazer, M. Kherallah, Rifampicin as Adjunct to Colistin Therapy in the Treatment of Multidrug-Resistant Acinetobacter baumannii, Ann. Pharmacother. 48 (2014) 766–771. doi:10.1177/1060028014528306.

Appendix A. Supplementary data

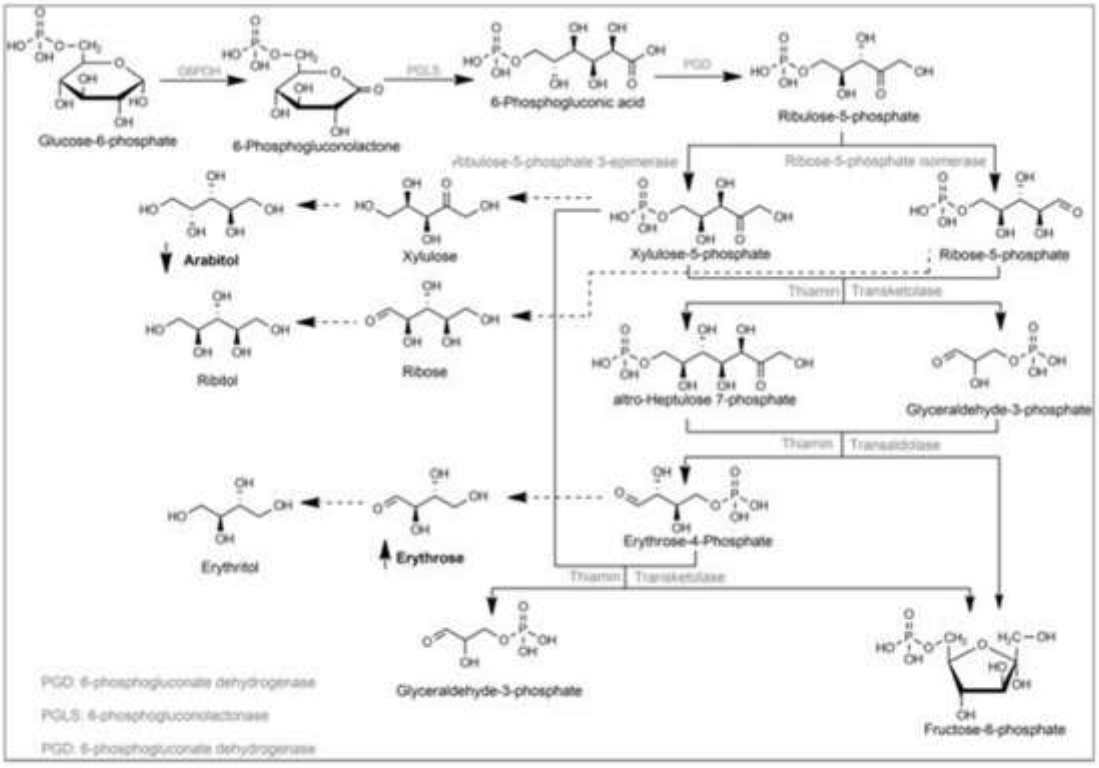

Figure: Pentose phosphate pathway indicating an elevated flux in the CMS treated *Mtb* towards glyceraldehyde-3-phosphate and fructose-6-phosphate, via the elevated erythrose and reduced arabinose concentrations.